

Seismic Performance Evaluation of Nonseismic Designed Flat-Plate Structures

Jinkoo Kim¹ and Taewan Kim²

Abstract: In this study the seismic performance of flat plate system structures designed without considering seismic load was investigated. Both the capacity spectrum method provided in ATC-40 in 1996 and nonlinear dynamic analyses were carried out to obtain maximum interstory drifts for earthquake loads. Also, a seismic performance evaluation procedure presented in FEMA-355F in 2000 was applied to evaluate the seismic safety of the model structures. The analysis results showed that the maximum interstory drifts of the nonseismic designed flat-plate structures computed by the capacity spectrum method and the nonlinear dynamic analysis were smaller than the limit state for the collapse prevention performance level. However, the results of the FEMA procedure showed that the model structures did not have enough strength to ensure seismic safety.

DOI: 10.1061/(ASCE)0887-3828(2008)22:6(356)

CE Database subject headings: Seismic design; Structural design; Plates.

Introduction

Flat-plate (FP) structures designed without considering seismic load may not have enough lateral strength and ductility to resist earthquake ground motions. In such structures column design is usually governed by axial loads, which results in a minimum amount of confinement steel and other undesirable detailing in columns to secure longitudinal reinforcing bars and a core concrete. Slabs in the vicinity of columns are designed for negative moment caused by vertical loads without shear reinforcement. These features of design may result in insufficient ductility of columns at large displacement and punching shear failure of slabs by unbalanced moment when subjected to earthquake loads. Currently, regulations for seismic design are changing toward increasing seismic forces and ductility of structural members, and therefore seismic retrofit of nonseismic designed old structures is becoming an emerging issue in many countries. In this regard the accurate prediction of FP structures, which are most vulnerable for lateral load, is important for proper retrofit of the structures.

Previous research on flat-slab or FP structures focused on the development of analysis methods (Sherif and Dilger 1998; Murray et al. 2003) and on the design or detailing techniques (Quisrani 1993; Dilger 2000; Kang and Wallare 2006). Recently, a significant amount of research has been devoted to the development of retrofit techniques for existing flat-slab/plate structures (Moehle 2000; Humay and Durrani 2001; Zhang et al. 2001; Bai 2003; Binici and Bayrak 2003). To develop appropriate retrofit methods for a structure, the seismic performance first needs to be

evaluated. For example, Hueste and Bai (2009a,b) evaluated seismic performance of reinforced concrete nonseismic designed FP structures. The perimeter moment frames were designed to resist the full lateral load in accordance with the codes used in St. Louis in the early 1980s. They found that the FP structures designed in accordance with the old design code failed to satisfy the collapse prevention design objective for seismic event with 2% probability of occurrence in 50 years in the Memphis, Tenn. area.

For analysis of nonseismic FP structures with no shear reinforcement in slabs, punching shear failure should be considered. Heuste and Wight (1999) introduced a punching failure model and analyzed an FP building designed only for gravity load; however in their study punching failure did not significantly affect the overall behavior of the building because there were perimeter frames designed to be a lateral load resisting system.

In this paper both deterministic and reliability-based methods were employed to evaluate the seismic performance of nonseismic designed FP structures. The deterministic method used is the capacity spectrum method (CSM) recommended in the ATC-40 (1996) and the reliability-based method is the confidence level method (CLM) presented six FEMA (2000a, b). Both methods were applied and compared to estimate the reliability of the structures for seismic load. In order to apply the evaluation methods, three- and six-story FP structures, which are assumed to be located in Korea, were designed without considering seismic loads, and nonlinear static and dynamic analyses were implemented with analytical models of the structures. The applied earthquakes are hazards with a 2,400 year return period specified in the Korea Building Code (Architectural Institute of Korea 2005).

Design and Modeling of Model Structures

Design of FP Structures

For analysis, model structures of three- and six-story reinforced concrete flat-plate structures with three bays in both directions as shown in Fig. 1 are prepared. The three-story structure was designed only for gravity load, and the six-story structure was de-

¹Associate Professor, Dept. of Architectural Engineering, Sungkyunkwan Univ., Suwon, Korea. E-mail: jkim12@skku.edu

²Assistant Professor, Division of Architecture, Kangwon National Univ., Chuncheon, Korea.

Note. Discussion open until May 1, 2009. Separate discussions must be submitted for individual papers. The manuscript for this paper was submitted for review and possible publication on December 27, 2007; approved on June 6, 2008. This paper is part of the *Journal of Performance of Constructed Facilities*, Vol. 22, No. 6, December 1, 2008. ©ASCE, ISSN 0887-3828/2008/6-356-363/\$25.00.

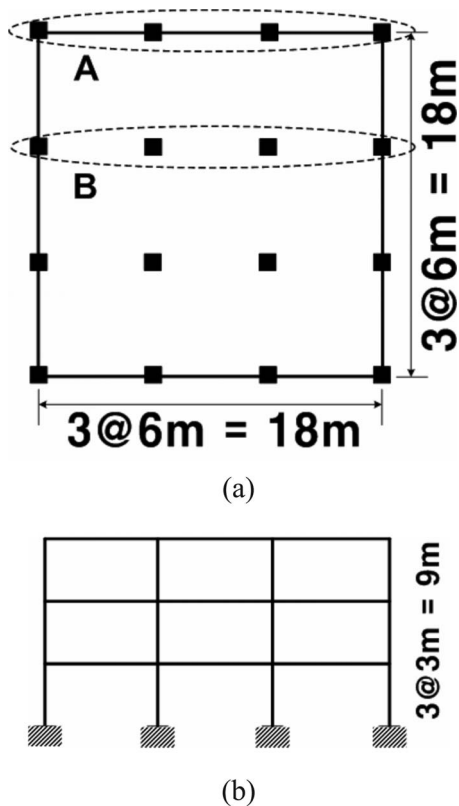


Fig. 1. Example buildings: (a) plan; (b) elevation view of three-story structure

signed for both gravity and wind loads. The design dead and live loads are 1.5 and 2.5 kN/m², respectively. The compressive strength of concrete is 20 MPa, and the tensile strength of reinforcing steel is 400 MPa. Following conventional design practice the same members were used in three consecutive stories. Slab thickness is 230 mm for both the three- and six-story structures, which satisfies the two-way punching shear failure criteria required in ACI 318-02 (2005). All columns were designed with identical size and reinforcement even though applied gravity loads are not identical at various locations (e.g., corner, exterior, or interior). Table 1 presents the member size and reinforcement of columns in the model buildings.

Modeling of FP Structures

As the prototype structures have regular floor plans, two-dimensional analytical models were used for seismic performance evaluation. The seismic performance of the analysis models was evaluated by nonlinear static and dynamic analyses using the program code OpenSees (Mazzoni et al. 2006). An exterior and an interior frame marked as A and B, respectively, in Fig. 1 were linked with rigid links as shown in Fig. 2 in such a way that only lateral forces and displacements are transmitted between frames.

Table 1. Member Size and Reinforcement of Columns in Example Structures (mm)

| Story | Size | Reinforcement |
|-------|-----------|----------------------|
| 3 | 400 × 400 | 8-D22 (D10 at 300) |
| 6 | 500 × 500 | One to three stories |
| | | Four to six stories |

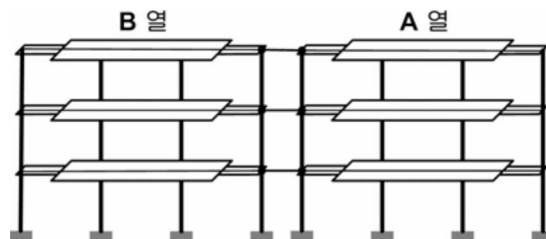


Fig. 2. Analytical modeling of the three-story flat-plate structure

The effective width of beams in the equivalent two dimensional frames was determined by formulas based on the research of Luo and Durrani (1995a, b). Dimensions and reinforcement of effective beams in the model structures are presented in Table 2.

As mentioned earlier, punching shear failure was modeled for slabs, which is expressed as equivalent beams. The parameters for including the effect of punching shear failure, which are presented in Table 3, are obtained by the procedure of Heuste and Wight (1999). Allowable rotations (θ_{allow}) in the equivalent beams are the rotations when punching shear failure starts in slabs, and they depend on the gravity shear ratio, which is the ratio of the applied shear by gravity load (V_g) to punching shear capacity of the slab (V_c), which is specified in ACI 318 (2005). The relationship between the gravity shear ratio and the allowable rotation for the three-story model structure is shown in Fig. 3.

For columns, concrete and reinforcing steel are modeled separately, and the concrete model is divided into cover and core concrete, which denote conventional and confined concrete. In the core concrete, confining effect of hoop steel was considered using the modified stress-strain relationship proposed by Mander et al. (1988). Figs. 4 and 5 depict the modeling of columns and the stress-strain relationship of the core concrete and reinforcing steel, respectively, in OpenSees. The concrete is divided into a number of layers, whereas the reinforcing bars are modeled as a single layer. For slabs, a plastic hinge model at each end of the equivalent beam is used to simulate the punching shear failure. The hysteretic behaviors of a column and an equivalent beam in the three-story structure induced by a cyclic load are shown in Fig. 6.

Definition of Limit State for Seismic Performance Evaluation

In order to apply the CSM and the CLM, proper definition of limit states is most important. In the CSM, the performance point on

Table 2. Dimensions and Reinforcement of Effective Beams in Example Structures (mm)

| Story | Frame | Bay | Effective width | Reinforcement | |
|-------|-------|----------|-----------------|---------------|--------|
| | | | | Top | Bottom |
| 3 | A | Interior | 1,500 × 230 | 11-D13 | 3-D13 |
| | | Exterior | 1,200 × 230 | 5-D13 | 2-D13 |
| | B | Interior | 3,000 × 230 | 22-D13 | 5-D13 |
| | | Exterior | 2,400 × 230 | 10-D13 | 3-D13 |
| 6 | A | Interior | 1,850 × 230 | 13-D13 | 3-D13 |
| | | Exterior | 1,500 × 230 | 6-D13 | 3-D13 |
| | B | Interior | 3,700 × 230 | 26-D13 | 5-D13 |
| | | Exterior | 3,000 × 230 | 12-D13 | 5-D13 |

Table 3. Parameters for Punching Shear Modeling of Equivalent Beams

| Story | Frame | Bay | V_g (kN) | V_c (kN) | V_g/V_c | Interstory | |
|-------|-------|----------|---------------|---------------|-----------|--------------|---------------------------|
| | | | | | | drift (%) | θ_{allow} (rad) |
| 3 | A | Interior | 151.4 | 507.1 | 0.30 | 2.75 | 0.035 |
| | | Exterior | 74.8 | 316.2 | 0.24 | 3.41 | 0.052 |
| | B | Interior | 304.8 | 763.8 | 0.40 | 1.50 | 0.010 |
| | | Exterior | 151.4 | 507.1 | 0.30 | 2.75 | 0.035 |
| 6 | A | Interior | 150.3 | 666.8 | 0.23 | 3.40 | 0.060 |
| | | Exterior | 73.9 | 378.8 | 0.20 | 4.00 | 0.071 |
| | B | Interior | 303.7 | 889.1 | 0.34 | 2.20 | 0.029 |
| | | Exterior | 150.3 | 666.8 | 0.23 | 3.40 | 0.060 |

the capacity curve should be inside the demand spectrum, and in the CLM, the capacity should be determined to be bounded by the limit state. The limit state adopted from FEMA 273 (1997) is the Collapse Prevention limit state in which a structure is in a state of imminent collapse, i.e., the structure is almost collapsed but standing. In both analysis methods, the limit state pairs with an earthquake hazard level, which is 2% probability of exceedance in 50 years (2/50 event). The limit state is usually defined using interstory drift because it can represent the damage state of structures well and is simple to use. An interstory drift limit of the structure, which is defined as a limit state at the system level, can be derived from the limit state of members, which is defined as a limit state at the element level. In this study, for both the CSM and the CLM, the interstory drift limit in system level is used as a parameter for evaluating the damage state of the model structures.

Limit State in Element Level

For the limit state of slabs, acceptance criteria of FEMA 356 (2000a) and the punching shear model of Heuste and Wight (1999) are adopted for slabs without shear reinforcement, which are shown in Fig. 7. In the FEMA criteria, a and b are identical and c is equal to zero, which implies that strength and ductility are not allowed after rotation reaches 0.02 rad. Punching shear model for the interior slab dictates that $\theta_{allow}=0.01$ rad and there is no ductile behavior after yield. For the limit state of columns, maximum strain of 0.01 in the core concrete is utilized (Mander et al. 1988).

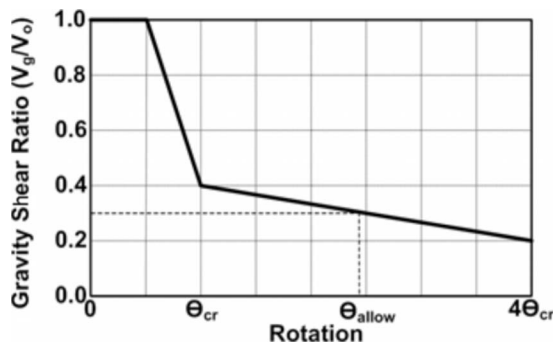


Fig. 3. Gravity shear ratio versus allowable rotation of slab

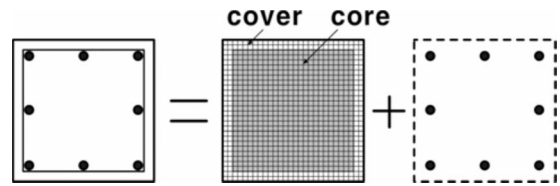


Fig. 4. Modeling of columns in OpenSees

Limit State at the System Level

The incremental dynamic analysis (IDA) summarized in Vamvatsikos and Cornell (2002) is used for determining the limit state of structures at the system level. The IDA was utilized to determine the global interstory drift limit in the SAC project Phase 2. The IDA is carried out such that maximum interstory drifts are checked at each step by incrementally increasing earthquake ground motions, then global limits are determined when the rate of drift change is larger than a certain level. The detailed procedure of the IDA is provided in the FEMA 355F (2000) and will also be described later in this paper. Another limit state at the system level is the interstory drift when maximum strain in core concrete of columns in any story exceeds 0.01. The results of push-over analysis showed that the maximum interstory drifts were 2.8 and 2.5% for the three- and the six-story structures, respectively. These were used as upper bounds of the limit state determined from the IDA.

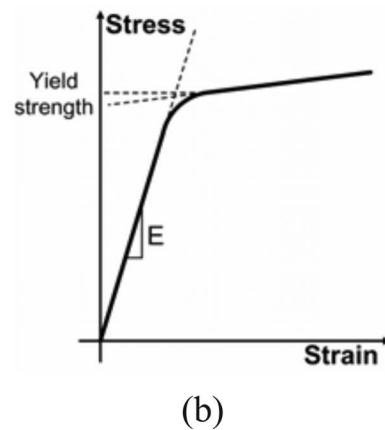
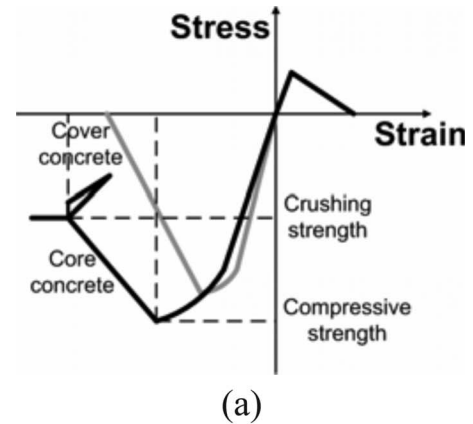
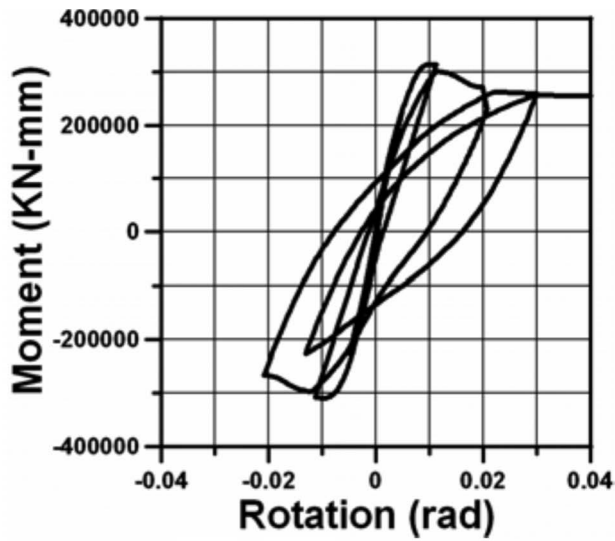
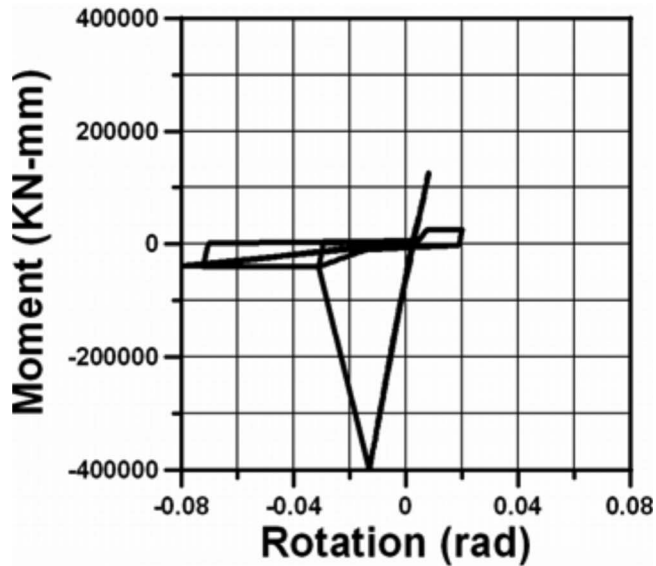


Fig. 5. Modeling of stress–strain relationship in OpenSees: (a) concrete; (b) reinforcing steel



(a)



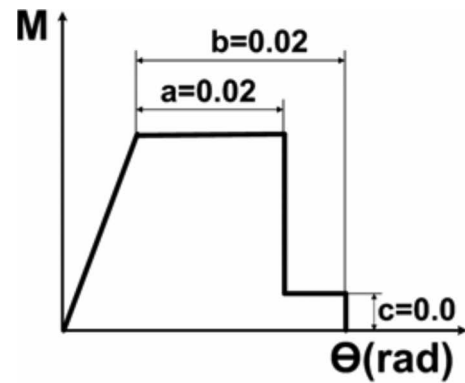
(b)

Fig. 6. Hysteretic behavior of structural members: (a) columns; (b) equivalent beams

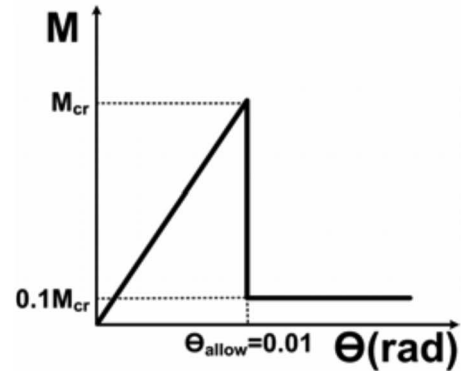
Performance Evaluation by Capacity Spectrum Method

Step-by-Step Procedure of Capacity Spectrum Method

The maximum displacements of the analysis models were computed based on the CSM presented in ATC-40 (1999). Although the CSM is an approximate method with many simplifications, it is a convenient tool for performance-based seismic evaluation, as it is based on nonlinear static analysis instead of on time-consuming nonlinear dynamic analysis. Application of the capacity spectrum technique requires that both the demand spectra and structural capacity curve be plotted in the spectral acceleration versus spectral displacement domain, which is known as the acceleration-displacement response spectra.



(a)



(b)

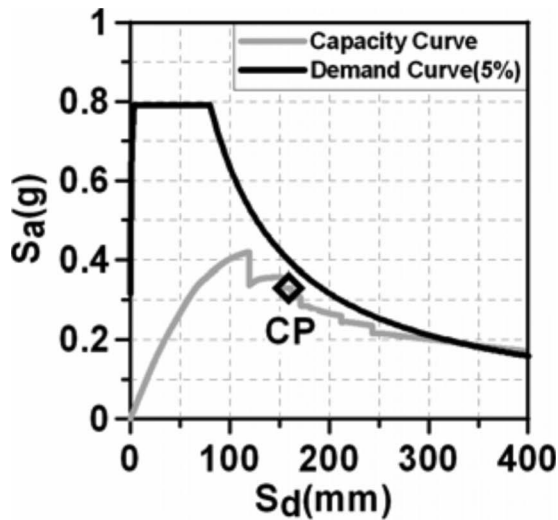
Fig. 7. Moment–rotation relationship in slabs of a flat plate structure: (a) FEMA criteria; (b) punching shear model for interior slab

A bilinear representation of the capacity spectrum is needed to estimate the effective damping and appropriate reduction of spectral demand. ATC-40 (1996) recommends that the area under the original capacity curve and the equivalent bilinear curve be equal so that the energy associated with each curve is the same. The equivalent viscous damping ratio for the yielding structure is determined from the energy dissipated by the hysteretic behavior and the stored potential energy at the maximum displacement. The effective damping ratio is obtained by combining the equivalent and the inherent viscous damping ratios, which is used to redraw the demand curve. From the new cross point of the capacity and demand curves, the effective damping ratio is recomputed and the demand curve is modified based on the new effective damping.

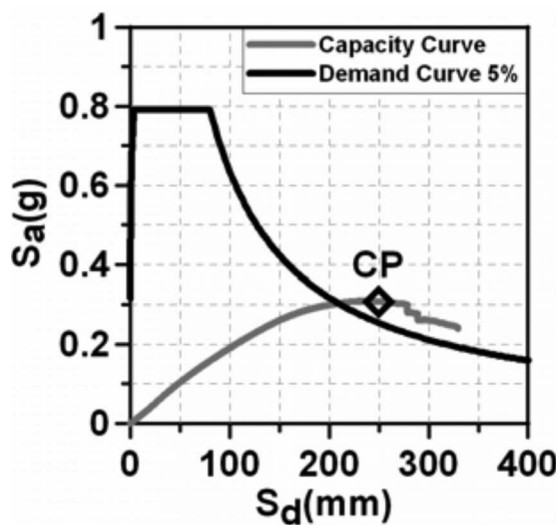
This process is continued until convergence and the final performance point is obtained from the cross point of the capacity and demand curves. The pseudoacceleration and displacement responses of the structure are computed by transforming the performance point of the equivalent single-degree-of-freedom system to that of the original multi-degree-of-freedom structure.

Performance Evaluation by Step-by-Step Procedure

Fig. 8 shows the capacity and demand curves of the model structures plotted in the spectral acceleration-displacement diagram. The capacity point (or limit state) determined from push-over analysis is denoted as CP in the Fig. 8. For the capacity curves, the storywise distribution of lateral load was determined to be proportional to the first mode of vibration. The demand curve is



(a)



(b)

Fig. 8. Capacity and demand curves of model structures: (a) three-story; (b) six-story

the design spectrum with the response spectral acceleration coefficients $S_{DS}=0.79$ and $S_{D1}=0.51$ in the International Building Code (ICC 2006) format, which is recommended in the Korea Building Code (Architectural Institute of Korea 2005) for seismic event of 2,400 year return period. It can be observed that the maximum lateral strength of the three-story structure is smaller than those required by the current seismic design code of Korea.

The process of estimating the effective damping ratio is summarized in Table 4, where the shaded line indicates the final converged value for effective damping. The variables S_{dy} and S_{ay} represent the maximum displacement and acceleration of the equivalent single-degree-of-freedom system, respectively, and S_{di} and S_{ai} represent the maximum displacement and the acceleration responses of the system. The final performance points and the inelastic responses of the analysis models are tabulated in Table 5. It can be seen that the maximum interstory drift of the three-story structure was 1.07% of the story height, which is smaller than the

Table 4. Effective Damping Ratio of Model Structures Obtained by the Capacity Spectrum Method

| ζ (%) | S_{dy} (mm) | S_{ay} (g) | S_{di} (mm) | S_{ai} (g) | ζ_{eff} (%) |
|-----------------------|------------------|-----------------|------------------|-----------------|----------------------|
| Three-story structure | | | | | |
| 17 | 55.5 | 0.369 | 82.7 | 0.371 | 18.17 |
| ⋮ | | | ⋮ | ⋮ | ⋮ |
| 18.9 | | | 79.2 | 0.359 | 18.94 |
| ⋮ | | | ⋮ | ⋮ | ⋮ |
| 20 | | | 75.5 | 0.361 | 17.28 |
| Six-story structure | | | | | |
| 10 | 110.3 | 0.233 | 165.3 | 0.2635 | 14.64 |
| ⋮ | | | ⋮ | ⋮ | ⋮ |
| 12.5 | | | 149.5 | 0.2549 | 12.57 |
| ⋮ | | | ⋮ | ⋮ | ⋮ |
| 15 | | | 136.1 | 0.2474 | 10.34 |

failure criterion of 2.8% presented earlier. In the six-story structure the maximum interstory drift is 1.44% of the story height, which is also less than the failure criterion, 2.5%. Consequently, the FP structures are considered to be safe based on the procedure of the CSM.

Nonlinear Dynamic Analysis

Nonlinear dynamic analyses of the analysis models were carried out using two artificial earthquake records and the ten earthquakes (Nos. 41–50) used in the SAC Project Phase 2 Somerville et al. (1997), which are seismic events with 50% probability of exceedence in 50 years in the Los Angeles area. Two artificial records were generated using the program SIMQKE (Vanmarcke and Gasparini (1976) 1976) in such a way that their response spectra fit the design spectrum of the Korean Building Code (Architectural Institute of Korea 2005). The other ten earthquakes were scaled to the seismic events with 2,400 year of return period in Korea. Table 6 presents the maximum roof displacements and the interstory drifts of the analytical model. It can be observed that the analysis results vary significantly depending on the earthquake record used. Even for the artificial records, which were generated based on the smooth design spectrum, the results did not match with those from the CSM. Therefore, the performance points obtained from the CSM may not represent the nonlinear behavior of a structure properly. Further, variation of results arising from randomness of earthquake ground motions needs to be considered for accurate seismic performance evaluation.

Performance Evaluation by Confidence Level Method

For thorough investigation of the seismic performance of the model structures, the reliability-based performance evaluation procedure, the CLM presented in FEMA 355F (2000b), was applied. In the procedure, randomness and uncertainty associated with predicting the capacity and demand are explicitly accounted for. The procedure was originally developed for evaluation of steel structures; Yun et al. (2002) and Lee and Foutch (2002a,b) carried out seismic performance evaluation of steel moment frames based on the procedure. The specific criteria for perfor-

Table 5. Performance Points of Model Structures Obtained by CSM

| Story | Equivalent SDOF | | MDOF | | | |
|-------|------------------------|------------------|------------------------|----------------------|------------------|--------------------------|
| | Roof displacement (mm) | Acceleration (g) | Roof displacement (mm) | Interstory drift (%) | Shear force (kN) | ζ_{eff} (%) |
| 3 | 79.2 | 0.359 | 100.1 | 1.07 | 1,044.9 | 18.9 |
| 6 | 149.5 | 0.255 | 193.3 | 1.44 | 1,419.8 | 12.6 |

mance evaluation requires the selection of a performance objective and a degree of confidence that the performance will not be worse. The FEMA procedure recommends that the global collapse prevention performance level is satisfied for 2/50 seismic hazard level. A 95% confidence in achieving this performance objective is also recommended.

Basic Frameworks for Acceptance Criteria

The acceptance criteria for the reliability-based procedure may be written in equation form as

$$\lambda = \frac{\phi \hat{C}}{\gamma \gamma_a \hat{D}} \quad (1)$$

where \hat{D} =estimate of median drift demand; \hat{C} =estimate of median drift capacity; ϕ =resistance factor; γ =demand factor; γ_a =analysis demand factor; and λ =confidence factor used to determine the confidence level. \hat{D} is the median estimate of the demand drift calculated using the appropriate hazard level response spectrum. \hat{C} is the median estimate of the capacity determined using the previously described method. Therefore, in the confidence factor, numerator and denominator represent capacity and demand of a system, respectively. The other factors, which are resistance, demand, and analysis demand factors, are included to consider uncertainty in estimating the medians. The resistance factor is less than 1.0 and the demand and analysis demand factors are larger than 1.0, so that each acts on decreasing the median capacity and increasing the median demand. A more detailed derivation of these equations is given by Jalayer and Cornell (2003) and Cornell et al. (2002). In the CLM, confidence level is determined by estimating the confidence factor and other parameters utilizing Tables 5–6 in the FEMA 355F (2000b).

Reliability-Based Performance Evaluation

For evaluation process, a set of 20 earthquake records (LA 41–60) used in the SAC project (Somerville et al. 1997) were applied. These records were scaled to fit the design spectrum of the Korean Building Code (Architectural Institute of Korea 2005) 2,400 year return period—as mentioned before. In order to determine the drift capacity, the (IDAs) were carried out with the following procedures:

1. Scale the earthquake records so that the pseudoacceleration S_a at the period of the structure becomes 0.1 g.
2. Estimate the maximum interstory drift of the structure by carrying out nonlinear dynamic analyses.
3. Increase S_a by 0.1 g and carry out the nonlinear dynamic analysis.
4. Obtain the maximum interstory drift when the slope of the IDA curve becomes less than 20% of the initial (elastic) slope, which is the capacity of the structure.

As mentioned before, the maximum drift obtained from the push-over analysis was used as an upper bound. Fig. 9 presents some IDA results of the three- and the six-story structures. For the most cases, the drift capacities were determined by the upper bound limit values, which are represented by vertical lines in Fig. 9.

Uncertainties in estimation of strength of concrete and reinforcing steel and natural period, which is related to the stiffness of material, were considered for determination of the analysis demand factor. For consideration of the uncertainties, mean and standard deviation of the variables are necessary. The nominal strength used for design of model structures was 20 and 400 MPa for concrete and reinforcing steel, respectively. For strength of concrete, the mean value and coefficient of variation (COV) were taken as 25 MPa and 15%, respectively. For strength of reinforcing steel, the mean and COV were taken as 475 MPa and 6%, respectively. These values were adopted from Erberik and Elnashai (2004). The mean natural periods of the model buildings were computed from the analyses of the model structures using nominal elastic moduli of concrete and reinforcing steel. Due to lack of data for FP structures, the standard deviation of the natural periods of FP structures, 0.29 s, obtained from Kim and Kim (2007) for reinforced concrete moment frames, was adopted.

For utilizing Tables 5–6 in the FEMA 355F (2000b), the slope of the hazard curve, k , was computed as follows:

$$k = \ln \left[\frac{H_{s_a-10\%}}{H_{s_a-2\%}} \right] / \ln \left[\frac{S_{a-2\%}}{S_{a-10\%}} \right] \quad (2)$$

where $H_{s_a-10\%}$ and $H_{s_a-2\%}$ represent the probability of exceedance in 50 years, for which 1/474 and 1/2,475 were used, respectively. $S_{a-2\%}$ and $S_{a-10\%}$ represent the spectral acceleration in design code, and the ratio of $S_{a-2\%}$ and $S_{a-10\%}$ was 2.0 in this study. These lead to the slope of the hazard curve, k , of 2.4.

The results of the reliability-based analyses are presented in Table 7 for the three- and the six-story structures, respectively,

Table 6. Dynamic Analysis Results of Model Structures

| Variable | Three-story | | Six-story | |
|--------------|--------------------------------|------------------------------|--------------------------------|------------------------------|
| | Maximum roof displacement (mm) | Maximum interstory drift (%) | Maximum roof displacement (mm) | Maximum interstory drift (%) |
| Artificial 1 | 107.8 | 1.40 | 164.7 | 1.34 |
| Artificial 2 | 103.0 | 1.34 | 154.1 | 1.23 |
| LA (medium) | 111.5 | 1.58 | 152.4 | 1.25 |
| LA (max.) | 336.9 | 4.62 | 366.1 | 3.10 |
| LA (min.) | 51.0 | 0.69 | 57.9 | 0.45 |

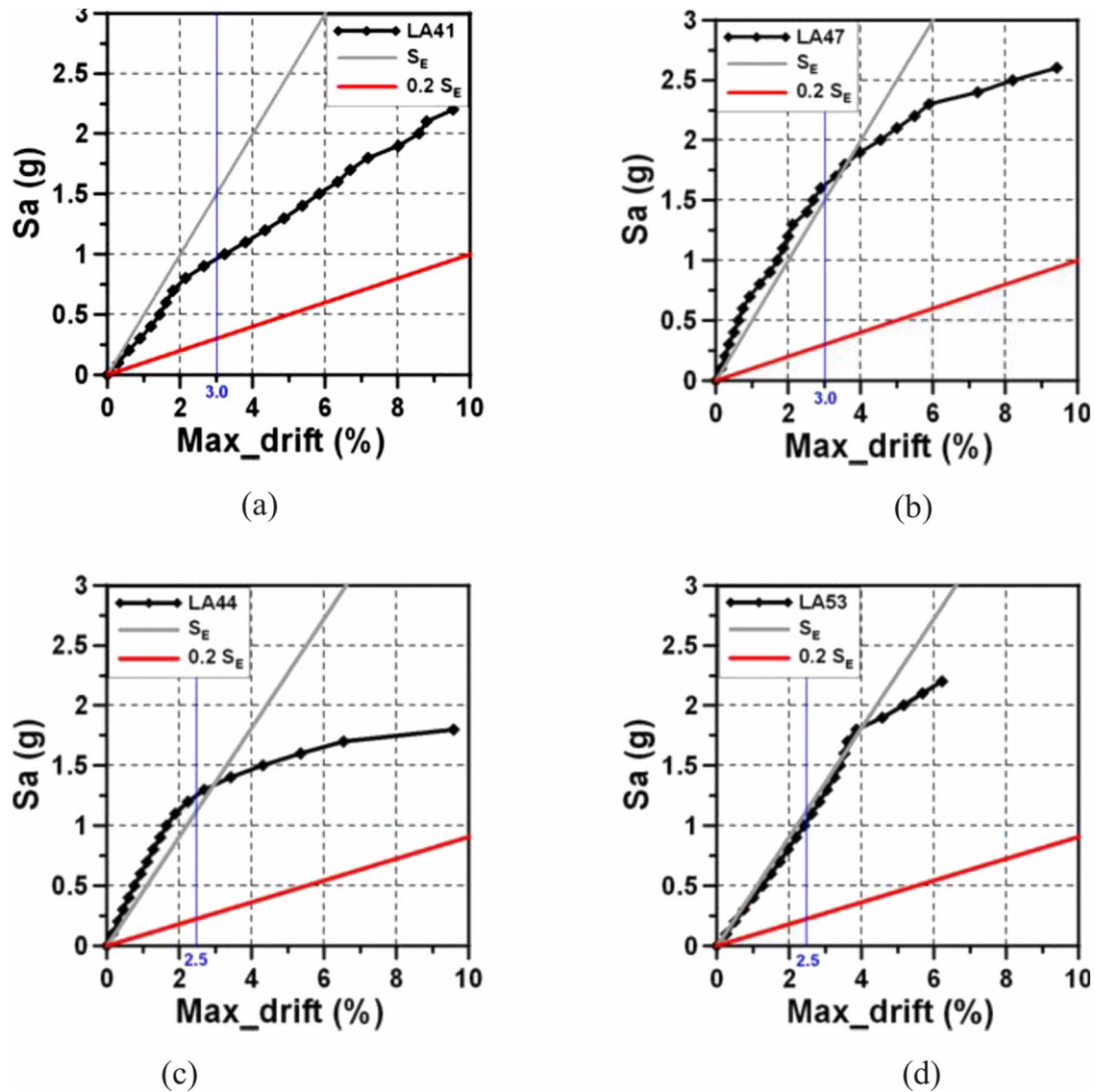


Fig. 9. Samples of IDA curves: (a) three-story (LA41); (b) three-story (LA47); (c) six-story (LA44); and (d) six-story (LA53)

where it can be observed that the confidence factors are 1.14 and 1.20, respectively. Based on Table 5-6 of FEMA 355F (2006) the confidence of the model structures was estimated to be 80 and 82% for the three- and the six-story structures, respectively. As both structures had reliability less than 90%, they failed to satisfy the performance criteria for seismic safety.

Table 7. Results of Confidence Level Method

| Variables | | Three-story | Six-story |
|-------------------|------------------------|-------------|-----------|
| Capacity side | Resistance factor | 0.86 | 0.86 |
| | Median capacity | 0.028 | 0.025 |
| Demand side | Demand factor | 1.42 | 1.42 |
| | Analysis demand factor | 1.11 | 1.10 |
| | Median demand | 0.013 | 0.011 |
| Confidence factor | | 1.227 | 1.203 |
| Total uncertainty | | 0.46 | 0.45 |
| Confidence level | | 83% | 82% |

Conclusions

In this study the seismic performance of flat plate structures designed without considering seismic load was investigated. The maximum interstory drifts of the model structures were obtained by nonlinear static (the capacity spectrum method) and dynamic analyses, and were compared with given performance criteria. The seismic performance was also evaluated by the confidence level method presented in FEMA-355F (2000b), which takes into account the uncertainty associated with the analysis.

The results from the capacity spectrum method showed that the interstory drift responses of the nonseismic designed flat-plate model structures subjected to earthquakes with return period of 2,400 years were less than the limit states defined in system level; however the reliability-based procedure of FEMA 355F (2000b) showed that the model structures failed to satisfy the performance criteria for seismic safety. It also should be mentioned that as the seismic performance of the model structures were evaluated based on the seismicity of Korea, which belongs to a low to medium seismic region, the performance of the nonseismic-

designed flat-plate structures built in high seismic regions will be worse than obtained in this paper.

Acknowledgments

This work was supported by Grant No. R0A-2006-000-10234-0 from the Basic Research Program of the Korea Science & Engineering Foundation. The writers appreciate this financial support.

References

- American Concrete Institute (ACI). (2005). "Building code requirements for structural concrete (ACI 318-95) and commentary (318R-95)." *ACI 318*, Farmington Hill, Mich.
- Applied Technology Council (ATC). (1996). "Seismic evaluation and retrofit of concrete buildings." *ATC 40*, Redwood City, Calif.
- Architectural Institute of Korea. (2005). *Korean building code*, Seoul, Korea.
- Bai, J. W. (2003). "Seismic retrofit for reinforced concrete building structures." *Consequence-Based Engineering Institute Final Rep.*, Texas A&M Univ., College Station, Tex.
- Binici, B., and Bayrak, O. (2003). "Punching shear strengthening of reinforced concrete flat plates using carbon fiber reinforced polymers." *J. Struct. Eng.*, 129(9), 1173-1182.
- Cornell, C. A., Jalayer, F., Hamberger, R. O., and Foutch, D. A. (2002). "Probabilistic basis for SAC Federal Emergency Management Agency steel moment frame guidelines." *J. Struct. Eng.*, 128(4), 526-533.
- Dilger, W. H. (2000). "Flat slab column connections." *Prog. Struct. Eng. Mater.*, 2(3), 386-399.
- Erberik, M. A., and Elnashai, A. S. (2004). "Fragility analysis of flat-slab structures." *Eng. Struct.*, 26(7), 937-948.
- Federal Emergency Management Agency (FEMA). (1997). "NEHRP guidelines for the seismic rehabilitation of buildings." *FEMA 273*, Washington, D.C.
- Federal Emergency Management Agency (FEMA). (2000a). "Prestandard and commentary for the seismic rehabilitation of buildings." *FEMA 356*, Washington, D.C.
- Federal Emergency Management Agency (FEMA). (2000b). "State of the art report on performance prediction and evaluation of steel moment-frame buildings." *FEMA 355F*, Washington, D.C.
- Hueste, M. B. D., and Bai, J. W. (2009a). "Seismic retrofit of a reinforced concrete flat-slab structure. Part I—Seismic performance evaluation." *Eng. Struct.*, in press.
- Hueste, M. B. D., and Bai, J. W. (2009b). "Seismic retrofit of a reinforced concrete flat-slab structure. Part II—Seismic fragility analysis." *Eng. Struct.*, in press.
- Hueste, M. B. D., and Wight, J. K. (1999). "Nonlinear punching shear failure model for interior slab-column connections." *J. Struct. Eng.*, 125(9), 997-1008.
- Humay, F. K., and Durrani, A. J. (2001). "Experimental study of perforated infill panels for retrofitting flat plates." *ACI Struct. J.*, 98(5), 727-734.
- International Code Council (ICC). (2006). *International building code*, Falls Church, Va.
- Jalayer, F., and Cornell, C. A. (2003). "A technical framework for probability-based demand and capacity factor design (DCFD) seismic formats." *PEER Rep. No. 2003/8*, Pacific Earthquake Engineering Center, Univ. of California at Berkeley, Berkeley, Calif.
- Kang, TH. K., and Wallace, J. W. (2006). "Dynamic responses of flat plate systems with shear reinforcement." *ACI Struct. J.*, 102(5), 763-773.
- Kim, T., and Kim, J. (2007). "Seismic performance evaluation of a RC special moment frame." *Struct. Eng. Mech.*, 27(6), 671-682.
- Lee, K., and Foutch, D. A. (2002a). "Performance evaluation of new steel frame buildings for seismic loads." *Earthquake Eng. Struct. Dyn.*, 31(3), 653-670.
- Lee, K., and Foutch, D. A. (2002b). "Seismic performance evaluation of pre-Northridge steel frame buildings with brittle connections." *J. Struct. Eng.*, 128(4), 546-555.
- Luo, Y. H., and Durrani, A. J. (1995a). "Equivalent beam model for flat-slab buildings—Part I: Interior connections." *ACI Struct. J.*, 92(1), 115-124.
- Luo, Y. H., and Durrani, A. J. (1995b). "Equivalent beam model for flat-slab buildings—Part II: Exterior connections." *ACI Struct. J.*, 92(2), 250-257.
- Mander, J. B., Priestley, M. J. N., and Park, R. (1988). "Theoretical stress-strain model for confined concrete." *J. Struct. Eng.*, 113(8), 1804-1826.
- Mazzoni, S., MacKenna, F., Scott, M. H., and Fenves, G. L. (2006). *OpenSees command language manual*, Pacific Earthquake Engineering Research Center, Berkeley, Calif., (<http://opensees.berkeley.edu>).
- Moehle, J. P. (2000). "State of research on seismic retrofit of concrete building structures in the U.S." *U.S.-Japan Symp. and Workshop on Seismic Retrofit of Concrete Structures—State of Research and Practice*, Japan Concrete Institute, Tokyo.
- Murray, K. A., Cleland, D. J., Gilbert, S. G., and Scott, R. H. (2003). "Improved equivalent frame analysis method for flat plate structures in vicinity of edge columns." *ACI Struct. J.*, 100(4), 454-464.
- Quisrani, A. N. (1993). "Interior post tensioned flat plate connections subjected to vertical and biaxial lateral loading." Ph.D. thesis, Dept. of Civil Engineering, Univ. of California at Berkeley, Berkeley, Calif.
- Sherif, A. G., and Dilger, W. H. (1998). "Analysis and deflections of reinforced concrete flat slabs." *Can. J. Civ. Eng.*, 25(3), 451-466.
- Somerville, P., Smith, N., Puntamurthual, S., and Sun, J. (1997). "Development of ground motion time histories for phase 2 of the FEMA/SAC steel project." *Background document, Rep. No. SAC/BD-97/04*, SAC Joint Venture, Richmond, Calif.
- Vamvatsikos, D., and Cornell, C. A. (2002). "Incremental dynamic analysis." *Earthquake Eng. Struct. Dyn.*, 31(3), 491-514.
- Vanmarcke, E. H., and Gasparini, D. A. (1976). "A program for artificial motion generation: User's manual and documentation." Dept. of Civil Engineering, Massachusetts Institute of Technology, Cambridge, Mass.
- Yun, S. Y., Hamburger, R. O., Cornell, C. A., and Foutch, D. A. (2002). "Seismic performance evaluation for steel moment frames." *J. Struct. Eng.*, 128(4), 534-545.
- Zhang, W. J., Teng, J. G., Wong, Y. L., and Lu, Z. T. (2001). "Behavior of two way RC slabs externally bonded with steel plates." *J. Struct. Eng.*, 127(4), 390-397.